

# Local-field excitations in 2D lattices of resonant atoms

S. N. Volkov and A. E. Kaplan

*Dept. of Electrical and Computer Engineering,  
Johns Hopkins University, Baltimore, MD 21218*

(Dated: February 12, 2010)

## Abstract

We study excitations of the local field (locsitons) in nanoscale two-dimensional (2D) lattices of strongly interacting resonant atoms and various unusual effects associated with them. Locsitons in low-dimensional systems and the resulting spatial strata and more complex patterns on a scale of just a few atoms were predicted by us earlier [A. E. Kaplan and S. N. Volkov, *Phys. Rev. Lett.* **101**, 133902 (2008)]. These effects present a radical departure from the classical Lorentz-Lorenz theory of the local field (LF), which assumes that the LF is virtually uniform on this scale. We demonstrate that the strata and patterns in the 2D lattices may be described as an interference of plane-wave locsitons, build an analytic model for such unbounded locsitons, and derive and analyze dispersion relations for the locsitons in an equilateral triangular lattice. We draw useful analogies between one-dimensional and 2D locsitons, but also show that the 2D case enables locsitons with the most diverse and unusual properties. Using the nearest-neighbor approximation, we find the locsiton frequency band for different mutual orientations of the lattice and the incident field. We demonstrate a formation of distinct vector locsiton patterns consisting of multiple vortices in the LF distribution and suggest a way to design finite 2D lattices that exhibit such patterns at certain frequencies. We illustrate the role of lattice defects in supporting localized locsitons and also demonstrate the existence of “magic shapes”, for which the LF suppression at the exact atomic resonance is cancelled.

PACS numbers: 42.65.Pc, 85.50.-n

## I. INTRODUCTION

In our recent Letter [1] we predicted nanoscale field patterns (*stratification*) emerging in one-dimensional (1D) arrays and two-dimensional (2D) lattices of strongly interacting atoms, driven by a radiation nearly resonant to the atomic transition. We predicted excitation of so called *locsitons* and a host of related effects. A general formulation of the problem and a more detailed theory for 1D arrays was presented in our most recent paper [2]. The present paper is an extension of [1, 2] toward the theory of *2D lattices* of resonant atoms, which produce a much richer set of effects. We construct here a detailed theory of interactions in the system by developing different 2D versions of the nearest-neighbor approximation (NNA), including the “near-ring” approximation (NRA). We also derive dispersion relations for various lattice-polarization configurations for all locsiton wave vectors within the corresponding first Brillouin zones. Our theory predicts such phenomena as subwavelength multicell patterns, including multivortex locsiton excitations, and locsitons localized near lattice defects. Further on, we predict “magic shapes” of nanosize groups of atoms, which reverse the effect of a resonant locsiton suppression present in all but few configurations. The simplest magic configuration which can be cut out of a triangular lattice is a six-point star with an atom at its center, which makes the lowest “magic number” of atoms to be 13.

The predicted effects would be totally unexpected within the standard theory of local fields [3] going back to the works of Lorentz [4] and Lorenz [5]. That celebrated theory asserts that the microscopic electric field  $\mathbf{E}_L$  acting upon any given atom in a medium—the *local* field (LF)—differs from the macroscopic field  $\mathbf{E}$  of the electromagnetic wave, because electric dipoles induced in neighboring atoms produce extra field to supplement the field of the incident wave. This difference is significant in dense media, where the interatomic interactions are sufficiently strong. Under such conditions, typical interatomic distances are much shorter than the optical wavelength, and the dipole-dipole interactions between atoms can be treated as quasistatic. The major point of the Lorentz-Lorenz theory (LLT) of local fields is that the LLT contains a fundamental assumption (which often remains implicit and unspoken in the literature) that the LF varies very insignificantly between neighboring atoms, much like the applied optical field on the subwavelength scale. Unsurprisingly, that theory results in the LF being proportional to the macroscopic electric field,  $\mathbf{E}_L = \mathbf{E}(\epsilon+2)/3$ , where  $\epsilon$  is the dielectric constant of the medium.

As we have shown in [1, 2], this assumption of the LF uniformity is not universally applicable; moreover, it completely falls apart when the uniformity of the atomic lattice is disturbed by impurities, boundaries, etc. Indeed, when the interatomic interactions are sufficiently strong and the system is not very large, highly nonuniform LF distributions emerge, resulting in a strong stratification of the LF and atomic excitations. This effect is best manifested in small-scale ordered arrays and lattices of atoms at near-resonance conditions, which allow to attain high interaction strength between neighboring atoms and to easily control it by tuning the laser frequency. We have shown [1, 2] that when the interaction with neighboring atoms becomes comparable to that with the external field, so that the interaction strength exceeds some critical value, the system will support LF excitations, which we call *locsitons*. In finite-size arrays and lattices, standing waves of locsitons may form nanoscale strata and complex patterns in the LF (and hence, in the induced atomic dipoles). A typical spacing between atoms in the arrays and lattices exhibiting the LF stratification is a few orders of magnitude shorter than the wavelength of light, so the quasistatic approximation of the standard LLT can still be used.

It is worth noting that locsitons are basically a linear phenomenon and can be excited by a weak incident field. We want to stress that locsitons, i. e., spatially nonuniform solutions, are not new stable-state alternatives to a presumably unstable uniform Lorentz solution at certain interaction parameters; the stability or instability of the solution is not an issue here. The emergence of locsitons is determined by the boundary conditions in a *finite structure*, so a locsiton is essentially *the only* physical solution, which thus replaces the uniform Lorentz solution. Absorption plays an important role here, as it directly affects spatial attenuation of locsitons and thus the maximum distance to a boundary, defect, or other inhomogeneity where locsitons can appear. In particular, as we have shown in [2], the size of an array that can support well pronounced locsitons is directly related to the characteristic absorption length. Locsitons vanish in the bulk of a crystal sufficiently far away from boundaries or defects.

Due to recent advances in fabricating nanoscale structures, the observation and practical applications of the LF nanostratification are becoming a reality. Theoretically, strongly interacting resonant particles discussed in [1] do not have to be atoms, but may also be quantum dots, molecules, clusters, etc. However, one has to remember that one of the major conditions for the structure to support the locsitons is that the interaction strength has

to exceed a critical value. Since this strength is proportional to the square of an individual dipole momentum and inversely proportional to the cube of the interparticle spacing and the linewidth of the particle resonance (see below), the atoms may become preferred candidates. A very high finesse of atomic resonances (i. e., their narrow linewidth), compared, for example, to plasmons (see below), also contributes greatly to the phenomenon, allowing one to see high-order locsiton resonances.

To observe locsitons, one has to create conditions to couple them efficiently to an optical or some other kind of a probe. In [1, 2] we suggested a few promising methods of locsiton detection. In particular, locsitons could be observed via size-related resonances in a scattering of laser radiation or via x-ray or electron-energy-loss spectroscopy.

There are many potential applications of locsitons; here we will mention two of them which were discussed in [1]. It was shown in [1] that in the presence of a sufficiently strong optical field (i. e., in the nonlinear case), the LF in 1D arrays of strongly coupled dipoles can exhibit optical bistability, which could be used to design nanoscale all-dielectric logic elements and switches. Such devices might complement currently used semiconductor-based electronic circuits. Another potential application of locsitons could be based on the extreme sensitivity of size-related locsiton resonances to the size and shape of the system. At the exact atomic resonance, the field is normally “pushed out” of the atomic system, unless it has a certain “magic shape” [1]. Consequently, such “magic structures” of atoms could find applications in designing nanoscale biosensors.

Removing the assumption of the LLT that the dipoles in the medium oscillate in lock-step with the incident electromagnetic wave is a substantial paradigm shift in the theory of light-matter interaction. Locsitons predicted within our broader approach are a new phenomenon, although we can provide some incomplete but illustrative analogies from other areas of physics. For example, short- and long-wavelength strata in [1] are reminiscent of ferromagnetic and antiferromagnetic arrangements of static magnetic dipoles in the Ising model. The LLT is, on the other hand, more similar to the mean-field approach of the Curie-Weiss theory for magnetic media [6]. The Ising model is known to have richer consequences than the Curie-Weiss theory. Our case is, however, substantially different and most of all, more versatile than the Ising model. Indeed, instead of being static, as in the Ising model, the atomic dipoles are induced by the applied optical field and can oscillate with arbitrary amplitude and phase. By their nature, locsitons may be classified as Frenkel

excitons [7], because there is no charge transfer between atoms and the dipole interaction is due to bound electrons. Some of the locsiton effects, first of all, wave resonances, may be viewed as analogues of other types of oscillations and waves in condensed matter, like plasmons and phonons [7], as well as low-dimensional effects, like surface plasmons [8, 9], size-related resonances in thin metal films [10] or long organic molecules [11], “quantum carpets” [12], arrays of pendulums or electronic circuits [2], etc. Approaching from another perspective, one can view the formation of a locsiton band as a Rabi broadening of the atomic resonance due to strong interatomic interactions, which is essentially similar to the band formation in solid-state theory. However, although all waves and oscillations may be said to have something in common, locsitons form a distinct new class of phenomena because of the nonconductive, dielectric, nature of their optical response and a strong coupling between atoms, which is needed for attaining dramatic size-related resonances, magic configurations, and other interesting effects. A separate issue outside of the scope of this paper is how the structures can be fabricated or arranged. One can envision placing the atoms in a controlled way on the surface of suitable dielectric materials; recent developments in the atomic- and ion-traps technology allow for arranging atoms in vacuum as 1D arrays and 2D “crystals” in the so called wire traps [13].

Our paper is structured as follows. In Sec. II we outline our problem and present some general formulas; for more details the reader should refer to our recent paper [2]. In Sec. III we describe locsitons in infinite, unbounded, 2D lattices of resonant atoms in the case when the incident field is polarized in the lattice plane. The equations for the LF and the dispersion relations for the locsitons are first obtained in the NRA and then in the more precise NNA. In Sec. IV we discuss effects that arise in finite 2D lattices, in particular, formation of 2D patterns of the LF, due to size-related locsiton resonances, and the “magic” cancellation of the resonant LF suppression. In Sec. V we describe 2D locsitons in the case when the incident field is normal to the lattice plane. Sec. VI summarizes main results of our paper.

## II. 2D LATTICES: GENERAL MODEL

Let us consider a 2D lattice of strongly resonant identical particles, which we will further call “atoms”. We will assume that, for the incident laser frequency  $\omega$  near their resonant frequency  $\omega_0$ , these atoms can be described by a two-level model with the transition dipole

moment  $d_a$ . In the linear case, i. e., when the laser intensity is significantly lower than the saturation intensity, the results for the two-level model coincide exactly with those for the classical harmonic oscillator, see [2]. We further only consider lattices of atoms interacting via quasistatic near-field dipole forces. In general, this assumption is valid if, on one hand, the minimum separation  $l_a$  between atoms is not too small, so that their atomic orbitals do not overlap, and, on the other hand, the lattice is finite and its overall dimensions are smaller than the laser wavelength  $\lambda$ . However, in most cases, in particular within the NNA, which is the most common one and used throughout this paper, the sufficient condition is much less restrictive, only requiring that the interatomic separation  $l_a \ll \lambda$ , which is the same limit as in the standard LLT [3].

The LF acting upon a given atom located at a point  $\mathbf{r}$  is a superposition of the incident (“external”) field  $\mathbf{E}_{\text{in}}$  and the sum of the fields  $\mathbf{E}_{\text{dp}}(\mathbf{r}, \mathbf{r}')$  from surrounding dipoles at all other lattice positions  $\mathbf{r}'$  over the entire lattice:

$$\mathbf{E}_{\text{L}}(\mathbf{r}) = \mathbf{E}_{\text{in}}(\mathbf{r}) + \sum_{\text{lattice}}^{\mathbf{r}' \neq \mathbf{r}} \mathbf{E}_{\text{dp}}(\mathbf{r}, \mathbf{r}'), \quad (1)$$

where the near fields of the surrounding atomic dipoles  $\mathbf{p}(\mathbf{r}')$  are dominated by the non-radiative (quasi-static) components [14],

$$\mathbf{E}_{\text{dp}}(\mathbf{r}, \mathbf{r}') = \frac{3\mathbf{u}[\mathbf{p}(\mathbf{r}') \cdot \mathbf{u}] - \mathbf{p}(\mathbf{r}')}{\epsilon|\mathbf{r}' - \mathbf{r}|^3}. \quad (2)$$

Here  $\mathbf{u} \equiv (\mathbf{r} - \mathbf{r}')/|\mathbf{r} - \mathbf{r}'|$  is a unit vector along the line connecting the two atoms,  $\epsilon$  is the background dielectric constant ( $\epsilon = 1$  in vacuum and  $\epsilon \neq 1$  if a host medium is present). The atomic dipoles  $\mathbf{p}(\mathbf{r}')$  are, in turn, induced by the LF acting upon them. In the case of linear optical response of a two-level atom, its induced dipole moment is

$$\mathbf{p}(\mathbf{r}) = -\mathbf{E}_{\text{L}}(\mathbf{r}) \frac{2|d_a|^2}{\hbar\Gamma(\delta + i)}, \quad (3)$$

where  $\delta \equiv T(\omega - \omega_0)$  is a dimensionless laser frequency detuning and  $T = 2/\Gamma$  is the transverse relaxation time of the atom with a resonant homogeneous linewidth  $\Gamma$ . The condition that the electron orbitals of neighboring atoms do not overlap implies that  $l_a \gg |d_a|/e$  and justifies our use of a semiclassical approach. Nonlinear effects in systems of resonant atoms could be included into this picture via the saturation nonlinearity of the two-level system. As we have recently demonstrated [1, 2], the nonlinearity enables interesting

effects with promising applications, like the optical bistability and hysteresis. In the present paper, however, we will only consider *linear* effects in 2D lattices of resonant atoms.

We can rewrite Eqs. (1)–(3) in the following closed form,

$$\mathbf{E}_L(\mathbf{r}) = \mathbf{E}_{\text{in}}(\mathbf{r}) - \frac{Q}{4} \sum_{\text{lattice}}^{\mathbf{r}' \neq \mathbf{r}} \frac{l_a^3}{|\mathbf{r}' - \mathbf{r}|^3} \times \{3\mathbf{u}[\mathbf{E}_L(\mathbf{r}') \cdot \mathbf{u}] - \mathbf{E}_L(\mathbf{r}')\}, \quad (4)$$

where we introduced the dimensionless strength  $Q$  of the dipole-dipole coupling between neighboring atoms, which is easily controlled through the normalized frequency detuning  $\delta$ ,

$$Q = \frac{Q_a}{\delta + i}. \quad (5)$$

The maximum normalized strength of interaction between neighboring atoms,

$$Q_a = \frac{8|d_a|^2}{\epsilon \hbar \Gamma_a^3}, \quad (6)$$

is reached at zero detuning of the incident laser frequency from the atomic resonance ( $\delta = 0$ ). Note that this is the point where our approach drastically departs from the conventional LF theory, where the LF is implied quasi-uniform on a scale of many  $l_a$ , so that  $\mathbf{E}_L(\mathbf{r}) \approx \mathbf{E}_L(\mathbf{r}')$ . More details on the general LF model that we use in this paper, including some quantitative estimates of  $Q_a$  for realistic systems, can be found in our recent publication [2].

In the present paper we restrict our considerations to the *nearest-neighbor approximation* (NNA), in which only interactions between the closest atoms are taken into account in Eq. (4). As we demonstrated in [1, 2], this approximation leads to qualitatively similar results compared to the full solution, that takes into account interactions between all pairs of atoms in the system. The NNA allows us to derive simpler analytic expressions and undertake numerical simulations for reasonably large lattices.

### III. LOCSITONS IN TRIANGULAR LATTICES: IN-PLANE POLARIZATION

In this section we consider the emergence and properties of locsitons in infinite unbounded planar lattices of atoms. Here we aim at studying locsitons in their “simplest” form, without the system boundaries complicating the picture. At the same time, we will continue to assume the near-field character of the interatomic interaction, because our ultimate goal is

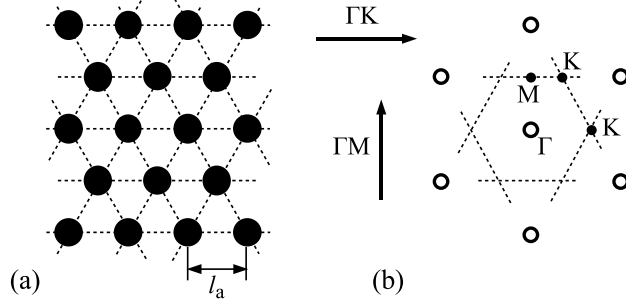


FIG. 1: (a) Geometry of an equilateral triangular lattice of resonant atoms. (b) The corresponding reciprocal lattice, shown with open circles, and some high-symmetry points and directions in the first Brillouin zone. The dashed lines in (b) illustrate constructing the first Brillouin zone as the Wigner-Seitz cell of the reciprocal lattice.

to study systems that are much smaller than  $\lambda$ . For the same reason, we will assume the incident field to be uniform throughout the lattice,  $\mathbf{E}_{\text{in}}(\mathbf{r}) \equiv \mathbf{E}_{\text{in}}$ , although our formalism is not limited to this case. As we have proven in [1, 2] for linear (1D) systems of interacting atoms, such an approach is indeed of a great help for understanding the locsitos' behavior.

We consider an equilateral triangular lattice (also known as a hexagonal lattice) of atoms, which has a six-fold rotation symmetry and belongs to the plane symmetry group (wallpaper group)  $p6m$ . [See Fig. 1(a).] This lattice type has a remarkable property of providing the most close-packed configuration of identical circular objects in a plane. Each atom in the lattice has six neighbors at the distances of  $l_a$ . The “second layer” of neighbors is removed by  $\sqrt{3}l_a$  or  $2l_a$ ; considering the fast decrease of the dipole-dipole interaction force with the distance ( $\propto 1/r^3$ ), the NNA which ignores interaction with the second and further layers of neighbors is expected to work well.

As in the case of 1D arrays of atoms [1, 2], two major cases can be studied separately, where the incident laser field  $\mathbf{E}_{\text{in}}$  lies *in plane* (the “ $\parallel$ ” case) or is *normal* to the plane of the lattice (the “ $\perp$ ” case). The linear optical response in the case of any other incident polarization can be obtained using a superposition of these two configurations. Of the two major cases, the “ $\parallel$ ” configuration is by far more interesting, exhibiting richer locsiton behavior and differing significantly from the 1D case due to the crucial in-plane anisotropy of the dipole-dipole interaction. It is also easier to implement, as the laser beam may be incident at the normal to the lattice of atoms, with the incident field being virtually uniform



on a scale of many wavelengths. The “ $\perp$ ” configuration presents a much closer analogy to the 1D problems considered in [1, 2], although some details inevitably differ. We will discuss it below in Sec. V. Further in this section, we only consider the “ $\parallel$ ” case, where both  $\mathbf{E}_{\text{in}}$  and  $\mathbf{E}_{\text{L}}$  lie in the lattice plain.

### A. Near-ring approximation

Optical response of a triangular lattice of atoms is, in general, anisotropic: it depends on the orientation of  $\mathbf{E}_{\text{in}}$  in the lattice plane with respect to the symmetry directions of the lattice. We have demonstrated, however, that one can use the near-ring approximation (NRA) to describe the behavior of long-wavelength locsitions in the lattice [1] in an isotropic fashion. In this approximation, the contribution from the surrounding dipoles to the LF  $\mathbf{E}_{\text{L}}$  [the second term in Eq. (1)] is substituted with a field from an effective dipole ring with the radius  $l_a$ , such that the polarizability of the nearest six atoms is evenly redistributed along the ring. The NRA is thus a further simplification of the NNA, making the model isotropic in the lattice plane. Within the NRA we then replace the summation in Eq. (4) with an integration over the imaginary ring, so that the equation for the LF becomes

$$\mathbf{E}_{\text{L}}(\mathbf{r}) = \mathbf{E}_{\text{in}} - \frac{3}{4\pi}Q \int_0^{2\pi} \mathbf{E}_{\text{L}}(\mathbf{r} + l_a\mathbf{u}) (3 \cos^2 \theta - 1) d\theta, \quad (7)$$

where  $\mathbf{u}$  is a unit vector in the direction from the center  $\mathbf{r}$  of the effective ring to a point at the ring, and  $\theta$  is the polar angle of  $\mathbf{u}$  counted from the direction of  $\mathbf{E}_{\text{in}}$  in the lattice plane. The strength of the dipole-dipole coupling between neighboring atoms is still given by the dimensionless parameter  $Q$  [Eq. (5)].

Equation (7) has a uniform (*Lorentz*) solution

$$\bar{\mathbf{E}}_{\text{L}} = \frac{\delta + i}{\delta - \delta_{\text{LL}} + i} \mathbf{E}_{\text{in}}, \quad (8)$$

where

$$\delta_{\text{LL}}^{\parallel} = -\frac{3}{4}Q_a \quad (9)$$

is the normalized frequency detuning at which the Lorentz-Lorenz resonance is achieved in the triangular lattice of atoms within the NRA. As we will see in Sec. V,  $\delta_{\text{LL}}$  is different for the “ $\parallel$ ” and “ $\perp$ ” configurations, but to simplify the formulas, we omit the index “ $\parallel$ ” everywhere in this section and in Sec. IV, except for Eq. (9). From Eq. (8) one can see that,

if  $|\delta_{LL}| \sim Q_a \gg 1$ , the uniform Lorentz LF is suppressed when the laser is tuned closely to the exact atomic resonance,  $\delta \approx 0$ , reaching its minimum intensity

$$|\bar{\mathbf{E}}_{\text{L}}|_{\text{min}}^2 \approx \frac{|\mathbf{E}_{\text{in}}|^2}{1 + \delta_{LL}^2}. \quad (10)$$

The LF in this case is effectively “pushed out” by the lattice atoms. Interestingly, a huge LF enhancement is reached at a red-shifted frequency, at  $\delta \approx \delta_{LL} < 0$ , where

$$|\bar{\mathbf{E}}_{\text{L}}|_{\text{max}}^2 \approx (1 + \delta_{LL}^2) |\mathbf{E}_{\text{in}}|^2. \quad (11)$$

Note that Eqs. (8), (10), and (11) are very similar to the corresponding equations for 1D arrays of atoms which were discussed in [1, 2]. The only difference is that the relation between  $\delta_{LL}$  and  $Q_a$  there was  $\delta_{LL} = -Q_a$  if  $\mathbf{E}_{\text{in}}$  is parallel to the array (and dipoles are aligned “head-to-tail”) and  $\delta_{LL} = Q_a/2$  if  $\mathbf{E}_{\text{in}}$  is perpendicular to the array (and dipoles are aligned “side-to-side”), assuming the NNA [see, e. g., Eq. (3.4) of Ref. [2]]. Here, within the NRA,  $\delta_{LL}$  does not depend on the incident field polarization in the lattice plane. Quite naturally, its value (9) lies in-between the two values for the 1D array, because mutual orientations of different pairs of dipoles in the lattice vary between the two extremes.

The frequency dependence of a *spatially uniform* LF, like in Eq. (8), and the associated Lorentz shift are long known phenomena. Similar effect was also observed experimentally in *alkali* vapors [15]. The unusual new phenomenon is that in ordered low-dimensional structures there are *spatially varying* solutions, which we call *locsitons* [1], that emerge at some values of  $Q$  in addition to the uniform LF. We will look for the locsitons in the form of 2D plane-wave excitations of the LF:

$$\Delta \mathbf{E}_{\text{L}} \propto \exp(i\mathbf{q} \cdot \mathbf{r}/l_a), \quad (12)$$

where  $\mathbf{q}$  is the normalized wave vector of the locsiton. By substituting  $\mathbf{E}_{\text{L}} = \bar{\mathbf{E}}_{\text{L}} + \Delta \mathbf{E}_{\text{L}}$  into Eq. (7) we obtain the dispersion relation for the wave vector  $\mathbf{q}$  in an integral form:

$$1 + \frac{3Q}{4\pi} \int_0^\pi (3 \cos 2\theta + 1) \cos[q \cos(\theta - \psi)] d\theta = 0, \quad (13)$$

where  $\psi$  is the polar angle of  $\mathbf{q}$  counted from the direction of  $\mathbf{E}_{\text{in}}$  in the lattice plane. Using the standard expansion of trigonometric functions with a harmonic argument into Bessel functions [see, e. g., Eq. (21.8-25a) in Ref. [16]],

$$\cos(q \sin \phi) = J_0(q) + 2 \sum_{m=1}^{\infty} J_{2m}(q) \cos(2m\phi), \quad (14)$$

where  $J_m(q)$  is the Bessel function of the first kind, we evaluate the integral in Eq. (13) in an explicit form and write Eq. (13) as

$$1 + \frac{3}{4}Q [J_0(q) - 3J_2(q) \cos(2\psi)] = 0. \quad (15)$$

By substituting  $Q$  from Eqs. (5) and (9), we can rewrite the last formula as an explicit dispersion relation connecting the normalized detuning  $\delta$  with the normalized locsiton wave vector  $\mathbf{q}$  which is represented by its polar coordinates  $q$  and  $\psi$ :

$$D_2^{\text{NRA}}(\mathbf{q}) \equiv J_0(q) - 3J_2(q) \cos(2\psi) = \frac{\delta + i}{\delta_{\text{LL}}}. \quad (16)$$

In the limit of low absorption, i. e.,  $|\delta_{\text{LL}}| \gg 1$ , the r. h. s. of Eq. (16) may be replaced with  $\delta/\delta_{\text{LL}}$ . A more detailed analysis of the dispersion relation shows that spatial oscillations—locsitons with almost real  $\mathbf{q}$ —emerge in a limited frequency band around  $\omega_0$  with a normalized bandwidth  $\sim |\delta_{\text{LL}}|$ . It is exactly the frequency range where the interaction between resonant atomic dipoles may become comparable to or much stronger than the effects of the external field  $\mathbf{E}_{\text{in}}$ . The dispersion dependence  $\delta/\delta_{\text{LL}} = D_2^{\text{NRA}}(\mathbf{q})$  in this case is shown in Fig. 2(a), where the external field is assumed to be aligned with the  $x$  axis. At every given laser frequency  $\omega$ , locsitons with a whole range of wave vectors  $\mathbf{q}$  may be excited. This set of  $\mathbf{q}$ , all having different orientations, is represented by an isoline for the respective  $\delta/\delta_{\text{LL}} = D_2^{\text{NRA}}(\mathbf{q})$  in Fig. 2(a). Recalling that  $\delta_{\text{LL}} < 0$  [see Eq. (9)], we may notice that solid isolines (red shaded areas) correspond to red-shifted laser frequencies ( $\omega < \omega_0$ ), while dashed isolines (blue shaded areas) correspond to blue-shifted frequencies. The non-circular shape of the isolines reflects the highly anisotropic dispersion dependence for locsitons in the 2D lattice in the case of short-wave locsitons. In particular, at any given normalized frequency detuning  $\delta$ , locsitons with different orientations of  $\mathbf{q}$  with respect to  $\mathbf{E}_{\text{in}}$  may have very different  $q$  and, consequently, different wavelengths. At the same time, because the NRA describes the lattice in an averaged way, the orientation of  $\mathbf{E}_{\text{in}}$  with respect to the lattice does not affect the result.

In the general case, especially when looking at the limitations on the size of the structure, one needs to consider complex locsiton wave vectors  $\mathbf{q} = \mathbf{q}' + i\mathbf{q}''$  in the dispersion relations (13) or (16), like it was done for 1D arrays of resonant atoms in [2]. This would allow to describe the dissipation of 2D locsitons, which is most prominent near the Lorentz resonance, and *evanescent* locsitons, which exist outside the locsiton band. One can also calculate the

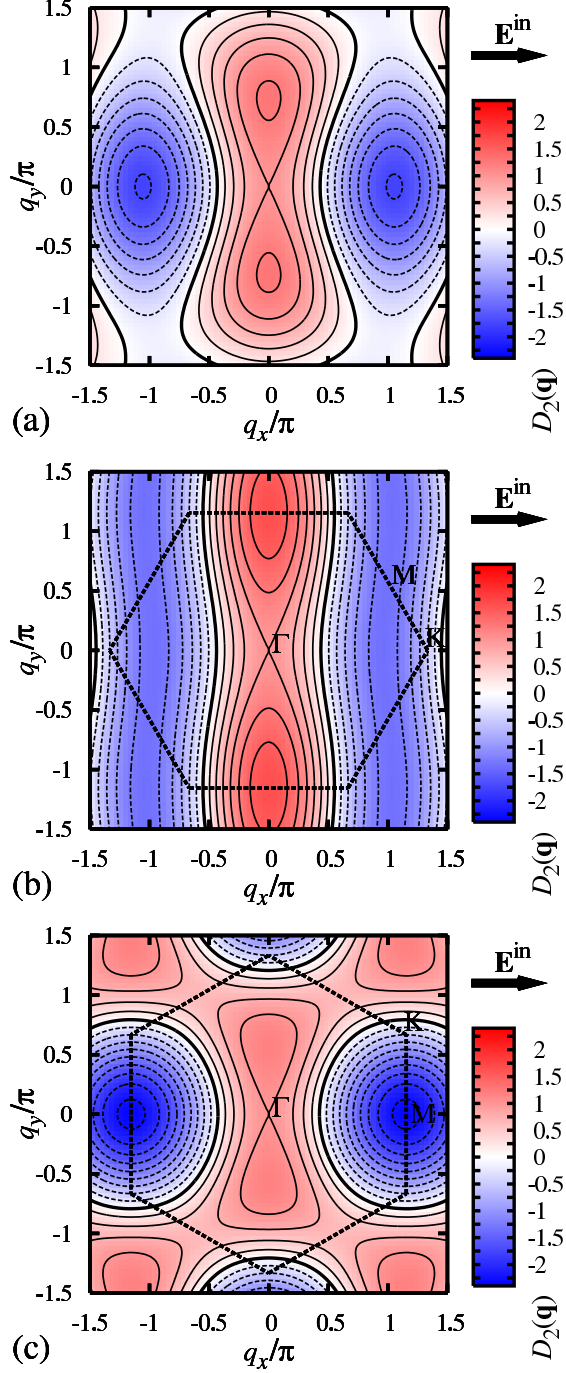


FIG. 2: (Color online) Dispersion dependences for locsitons in a triangular lattice of atoms (a) in the near-ring approximation; (b) for  $\mathbf{E}_{\text{in}} \parallel \Gamma K$ ; (c) for  $\mathbf{E}_{\text{in}} \parallel \Gamma M$ . Isolines of equal  $D_2(\mathbf{q})$  are spaced at 0.25 (i. e., they correspond to the ticks on the color bars); solid isolines and red shading correspond to positive  $D_2(\mathbf{q})$ , dashed isolines and blue shading correspond to negative ones, while the thicker solid isoline marks the zero level. The hexagons in plots (b,c) show the boundaries of the first Brillouin zone.

group velocity of the locsiton,  $\mathbf{v}_{\text{gr}} = (l_a/T)(d\delta/d\mathbf{q})$ , by taking a derivative of Eq. (16). Due to the anisotropy of Eq. (16), one may expect that the resulting dissipation and group velocity are highly dependent on the orientation of  $\mathbf{q}$  with respect to  $\mathbf{E}_{\text{in}}$ .

By its nature, the NRA only works well for long-wave locsitons, i. e., those with relatively small  $q$ . Indeed, for a long-wave locsiton, the LF at neighboring atoms differs insignificantly, so one may reasonably expect that replacing the neighboring dipoles at their actual positions with an effective dipole ring will not cause a significant change to the result. Our results obtained without resorting to the NRA (see Sec. III B), suggest that the NRA provides a good quantitative description of locsitons for  $q \lesssim \pi/2$ , while it gives reasonable *qualitative* estimates for  $q$  up to  $\sim \pi$ . One may use the two first terms from the Taylor series expansion to analyze Eq. (16) at small  $q$ , which is easy to do by recalling that  $J_0(q) = 1 - \frac{1}{4}q^2 + O(q^4)$  and  $J_2(q) = \frac{1}{8}q^2 + O(q^4)$  [cf. Eq. (21.8-3) in Ref. [16]], so that

$$D_2^{\text{NRA}}(\mathbf{q}) \approx 1 - \frac{1}{8}q^2[2 + 3 \cos(2\psi)] + O(q^4). \quad (17)$$

In the long-wavelength limit,  $D_2^{\text{NRA}}(\mathbf{q} = \mathbf{0}) = 1$  is reached at  $\delta = \delta_{\text{LL}}$ , yielding the uniform, Lorentz, solution for the LF. The second term in the r. h. s. of Eq. (17) indicates that the anisotropy with respect to the locsiton polarization shows up even at very small  $q$ , where Eqs. (16) and (17) can be rewritten as

$$q^2 = -\frac{8}{2 + 3 \cos(2\psi)} \frac{(\delta - \delta_{\text{LL}}) + i}{\delta_{\text{LL}}}. \quad (18)$$

Note that in describing locsitons at very small  $q$  (i. e., for  $\delta \approx \delta_{\text{LL}}$ ), the imaginary unit in the last formula cannot always be neglected compared to  $\delta - \delta_{\text{LL}}$ . The locsiton dissipation in this case may become significant, depending on  $\delta_{\text{LL}}$ , and the necessity of considering complex  $\mathbf{q}$  could appreciably complicate calculations. We will not go into the details of this special case in the present paper.

In 1D arrays of atoms, the Lorentz resonance,  $\delta = \delta_{\text{LL}}$ , always coincides with one of the edges of the locsiton frequency band [1, 2]. In that case, when one tunes the frequency of the incident laser beam towards  $\omega_0$  from the side of the Lorentz resonance, locsitons with the longest wavelength emerge first very close to the Lorentz resonance. The locsiton wavelength subsequently decreases as we approach and move past  $\omega_0$ . In a 2D lattice, the Lorentz resonance lies *within* the locsiton band, which means that, when similarly tuning the laser frequency towards  $\omega_0$ , short-wave locsitons will be excited first. In particular,

locsitons with  $\psi \approx \pm\pi/2$  (i. e., nearly transverse locsitons) may be excited at  $\delta/\delta_{\text{LL}} > 1$ , and can be thus viewed as the “easiest to excite” on the Lorentz side of the band. On the opposite, “anti-Lorentz” side of the band, where  $\delta/\delta_{\text{LL}} \lesssim -1$ , nearly longitudinal locsitons with  $\psi \approx 0$  or  $\pi$  lie closer to the band edge and thus are easier to excite. The exact positions of the edges of the locsiton band cannot be found within the NRA, because minima and maxima of  $D_2^{\text{NRA}}(\mathbf{q})$  are reached at such  $\mathbf{q}$  where the NRA may only be used for qualitative estimates. The case of larger  $q$  is addressed when we go beyond the NRA in the next subsection.

### B. Locsitons in the first Brillouin zone

When going beyond the NRA, the orientation of  $\mathbf{E}_{\text{in}}$  within the lattice plane becomes an important factor, except for small  $q$ . Staying within the NNA, i. e., only taking into account the six nearest neighbors in Eq. (4) (but *individually*, instead of them being washed out over the ring, as in the NRA), we are still able to approach the problem analytically. The resulting equation is

$$\mathbf{E}_{\text{L}}(\mathbf{r}) = \mathbf{E}_{\text{in}} - \frac{Q}{4} \sum_{\mathbf{u}_{\text{K}}} \{3\mathbf{u}_{\text{K}}[\mathbf{E}_{\text{L}}(\mathbf{r} + l_a \mathbf{u}_{\text{K}}) \cdot \mathbf{u}_{\text{K}}] - \mathbf{E}_{\text{L}}(\mathbf{r} + l_a \mathbf{u}_{\text{K}})\}, \quad (19)$$

where  $\mathbf{u}_{\text{K}}$  denotes any of the six unit vectors pointing in the directions from the atom (located at  $\mathbf{r}$ ) to one of its nearest neighbors.

The uniform, Lorentz, solution of Eq. (19) is still given by Eq. (8) and (9), which supports the above-mentioned convergence of the NRA and NNA results at  $q \rightarrow 0$ . Spatially varying *locsiton* solutions are found as in the previous subsection by using the ansatz (12) in Eq. (19). The corresponding dispersion relation  $\delta(\mathbf{q})$  for locsitons in a 2D triangular lattice can be now written as

$$D_2^{\text{NNA}}(\mathbf{q}) \equiv \sum_{n=0}^2 \left( \cos 2\theta_n + \frac{1}{3} \right) \cos[q \cos(\theta_n - \psi)] = \frac{\delta + i}{\delta_{\text{LL}}}. \quad (20)$$

where  $\theta_n = \theta_0 + n\pi/3$ , and  $\mathbf{q}$  is represented by its polar coordinates  $q$  and  $\psi$ . The orientation of the lattice with respect to the incident field  $\mathbf{E}_{\text{in}}$  is described by  $\theta_0$ , which is the angle that one of the vectors  $\mathbf{u}_{\text{K}}$  makes with  $\mathbf{E}_{\text{in}}$  (the fact that  $\theta_0$  is not unique does not affect the result). The ultimate proof that the results of the NRA and the more precise NNA converge

for long locsiton wavelengths can be obtained by taking a Taylor series expansion of Eq. (20) at  $q \rightarrow 0$ . By only retaining terms up to the order of  $q^2$  and calculating all the necessary sums and products of trigonometric functions, we find that Eqs. (17) and (18) still hold in the NNA.

It is sufficient to find locsitons with  $\mathbf{q}$  lying within the first Brillouin zone of the reciprocal lattice, because any solutions with  $\mathbf{q}$  lying outside the first Brillouin zone are physically equivalent to them due to the discrete nature of our system. The dispersion relation  $D_2^{\text{NNA}}(\mathbf{q})$  in Eq. (20) also has the required symmetry and periodicity. It is common to use high-symmetry points in the first Brillouin zone to denote most interesting directions in the lattice [see Fig. 1(b)]. Note that in terms of  $\mathbf{u}_K$  we may write  $\Gamma K \parallel \mathbf{u}_K$  and  $\Gamma M \perp \mathbf{u}_K$ .

The dispersion dependence  $\delta/\delta_{\text{LL}} = D_2^{\text{NNA}}(\mathbf{q})$  in the case of  $|\delta_{\text{LL}}| \gg 1$  is shown in Fig. 2(b,c) for two different orientations of  $\mathbf{E}_{\text{in}}$  with respect to the lattice: in Fig. 2(b)  $\theta_0 = 0$  (i. e.,  $\mathbf{E}_{\text{in}} \parallel \Gamma K$ ), while in Fig. 2(c)  $\theta_0 = \pi/2$  (i. e.,  $\mathbf{E}_{\text{in}} \parallel \Gamma M$ ). The  $x$  axis on the plots is aligned with the external field  $\mathbf{E}_{\text{in}}$ ; the hexagonal boundaries of the first Brillouin zones are shown with thicker dashed lines. The central parts of all three plots in Fig. 2 are very similar, which reflects our finding that Eqs. (17) and (18) hold for long locsiton wavelengths within both NRA and NNA. At the same time, significant differences accumulate closer to the boundaries of the first Brillouin zone. Fig. 2(b,c) also show that for both orientations of  $\mathbf{E}_{\text{in}}$  the maxima and minima of  $D_2^{\text{NNA}}(\mathbf{q})$  are attained at the zone boundaries, specifically, at different M points.

To facilitate the comparison of the three plots in Fig. 2 and finding the edges of the locsiton band, the NNA dispersion dependencies for two high-symmetry directions are presented in Fig. 3 and compared to the the NRA result. For both longitudinal and transverse locsitons, Fig. 3 shows corresponding cross-sections of the three plots of Fig. 2. As we already noted earlier in this paper, the NRA result is only meaningful for  $q$  up to  $\sim \pi$ ; Fig. 3 suggests that it is a good approximation for the NNA result at  $q \lesssim \pi/2$ , regardless of the orientation of  $\mathbf{E}_{\text{in}}$  with respect to the lattice. It is instructive to give explicit analytic expressions for each of the four NNA-based dependencies in Fig. 3. The respective dispersion relations derived from Eq. (20) and the corresponding ranges for  $\delta/\delta_{\text{LL}}$ , obtained in the assumption that  $|\delta_{\text{LL}}| \gg 1$ , are as follows:

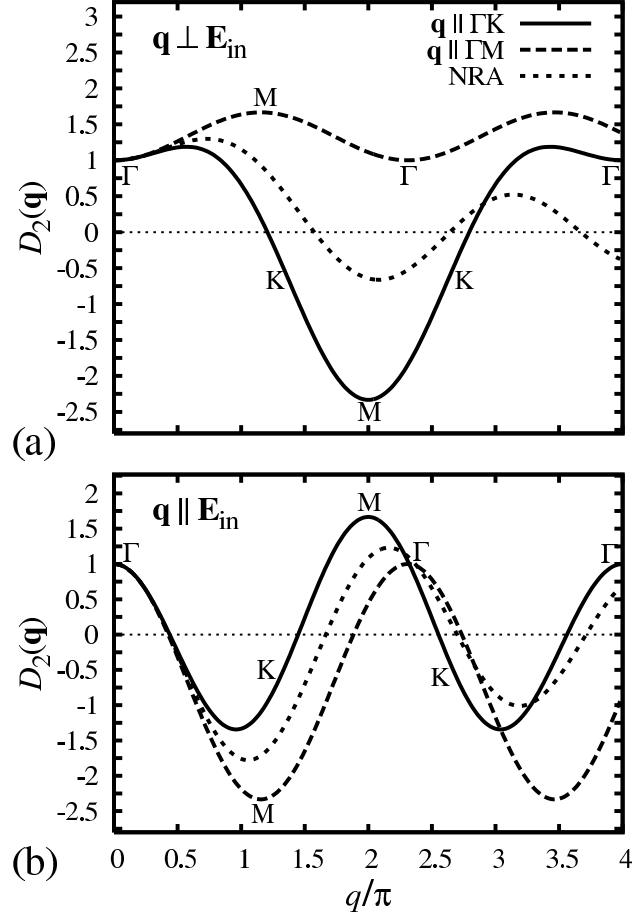


FIG. 3: Dispersion dependences for (a) transverse locsitons ( $\mathbf{q} \perp \mathbf{E}_{\text{in}}$ ) and (b) longitudinal locsitons ( $\mathbf{q} \parallel \mathbf{E}_{\text{in}}$ ) in a triangular lattice of atoms. Different curves correspond to the near-ring approximations (NRA) and the NNA for two different orientations of  $\mathbf{q}$  with respect to the lattice.

(a)  $\mathbf{E}_{\text{in}} \parallel \Gamma\text{K}$ ,  $\mathbf{q} \parallel \Gamma\text{M} \perp \mathbf{E}_{\text{in}}$  [long-dashed line in Fig. 3(a)],

$$\cos \frac{q\sqrt{3}}{2} = 4 - 3 \frac{\delta + i}{\delta_{\text{LL}}}, \quad (21)$$

$$1 \leq \frac{\delta}{\delta_{\text{LL}}} \leq 1\frac{2}{3}; \quad (22)$$

(b)  $\mathbf{E}_{\text{in}} \parallel \Gamma\text{M}$ ,  $\mathbf{q} \parallel \Gamma\text{K} \perp \mathbf{E}_{\text{in}}$  [solid line in Fig. 3(a)],

$$\cos \frac{q}{2} = \frac{1}{8} \left( 5 \pm \sqrt{57 - 48 \frac{\delta + i}{\delta_{\text{LL}}}} \right), \quad (23)$$

$$-2\frac{1}{3} \leq \frac{\delta}{\delta_{\text{LL}}} \leq 1\frac{3}{16}, \quad (24)$$

where the minimum of  $\delta/\delta_{\text{LL}}$  is reached outside the first Brillouin zone; this point more appropriately belongs to the case (d) below;



(c)  $\mathbf{E}_{\text{in}} \parallel \Gamma\text{K}$ ,  $\mathbf{q} \parallel \Gamma\text{K} \parallel \mathbf{E}_{\text{in}}$  [solid line in Fig. 3(b)],

$$\cos \frac{q}{2} = \frac{1}{16} \left[ 1 \pm \sqrt{1 + 32 \left( 4 + 3 \frac{\delta + i}{\delta_{\text{LL}}} \right)} \right], \quad (25)$$

$$-1 \frac{33}{96} \leq \frac{\delta}{\delta_{\text{LL}}} \leq 1 \frac{2}{3}; \quad (26)$$

where the maximum of  $\delta/\delta_{\text{LL}}$  is reached outside the first Brillouin zone, which point more appropriately belongs to the case (a);

(d)  $\mathbf{E}_{\text{in}} \parallel \Gamma\text{M}$ ,  $\mathbf{q} \parallel \Gamma\text{M} \parallel \mathbf{E}_{\text{in}}$  [long-dashed line in Fig. 3(b)],

$$\cos \frac{q\sqrt{3}}{2} = \frac{1}{5} \left( 2 + 3 \frac{\delta + i}{\delta_{\text{LL}}} \right), \quad (27)$$

$$-2 \frac{1}{3} \leq \frac{\delta}{\delta_{\text{LL}}} \leq 1. \quad (28)$$

The inequalities (24) and (26) also represent the edges of the locsiton bands for the cases of  $\mathbf{E}_{\text{in}} \parallel \Gamma\text{M}$  and  $\mathbf{E}_{\text{in}} \parallel \Gamma\text{K}$ , respectively (which explains our desire not to restrict the range of  $q$  to the first Brillouin zone when obtaining these inequalities). Note that locsitons with the largest red shift ( $\delta/\delta_{\text{LL}} > 0$ ) can be achieved with  $\mathbf{E}_{\text{in}} \parallel \Gamma\text{K}$ , while locsitons with the largest blue shift ( $\delta/\delta_{\text{LL}} < 0$ ) can be achieved with  $\mathbf{E}_{\text{in}} \parallel \Gamma\text{M}$ . Therefore, re-orienting the lattice with respect to the polarization of the incident laser beam may assist in controlling the type of locsitons excited in the lattice.

#### IV. FINITE LATTICES: IN-PLANE POLARIZATION

In this section, like in Sec. III, we only consider the case where  $\mathbf{E}_{\text{in}}$  is spatially uniform and lies in the lattice plane (the “||” case), which is easier to achieve if the laser beam is incident normally to the lattice plane. The presence of boundaries and defects in 2D lattices of resonant atoms can cause various locsionic effects, including giant LF resonances, formation of dipole strata, and “magic” cancellation of the resonant LF suppression. These effects are similar in their nature to their counterparts in 1D arrays of resonant atoms [1, 2], but their manifestations are much more diverse because of the inherent anisotropy of the dipole-dipole interaction in the 2D case, especially in the “||” geometry. Because of this, an all-encompassing study of finite 2D lattices is hardly possible within this pilot study on the subject, so we will restrict ourselves to providing some of the most characteristic results, which emphasize distinctions from the 1D problem.

### A. Size-related resonances and local-field patterns

Locsitons in a finite 1D array of atoms exhibit size-related resonances, characterized by large increases in their amplitudes at certain frequencies within the locsionic band, because locsitons are reflected at the boundaries and form standing waves (*strata*) [1, 2]. Essentially, these resonances correspond to locsiton eigenmodes defined by the boundaries. For the *long-wave strata* they are similar to oscillations of a quantum particle in a box, as, e. g., for 1D-confined electrons [10, 11], or a common violin string. It is natural to expect such resonances and eigenmodes to also exist in higher dimensions, in particular, in finite 2D lattices, where we also encounter locsiton reflections at the boundaries. An important distinction of the 2D case is that the wave vector  $\mathbf{q}$  of a locsiton may have an arbitrary orientation in the lattice plane with respect to the incident field  $\mathbf{E}_{\text{in}}$ . Multiple reflections and interference of locsitons with all possible  $\mathbf{q}$  quickly make the whole picture very complicated and highly susceptible to minor changes to the size and shape of the lattice patch. We found that at certain geometries only a limited number of locsiton eigenmodes are dominant. Their interference produces various dipole patterns and strata; some of them are reminiscent to “quantum carpets” [12]. An important issue is, therefore, how one can control the locsiton patterns via the geometry of the lattice patch and the frequency and polarization of the laser beam.

One way to engineer a distinct 2D locsiton pattern is to start with a rectangular lattice patch and ensure that size-related resonances are achieved for locsitons with wave vectors parallel to its boundaries. We have to choose the lattice shape, such that the size-related locsiton resonances emerge in both dimensions at the same frequency detuning  $\delta$ . To simplify our task, we will consider long-wavelength locsitons, which are not too sensitive to the system sizes and thus are easier to control, and, incidentally, also form more pronounced patterns and are described by the simpler formula (18).

In the limit of long-wavelength locsitons ( $q \ll 1$ ,  $\delta \approx \delta_{\text{LL}}$ ), the dispersion relations in the cases (a) and (b) described in Sec. III B coincide with each other:

$$q^2 = 8 \frac{(\delta - \delta_{\text{LL}}) + i}{\delta_{\text{LL}}} \quad (29)$$

[cf. Eq. (18) at  $\psi = \pi/2$ ]. In a similar manner, one obtains approximate solutions for the

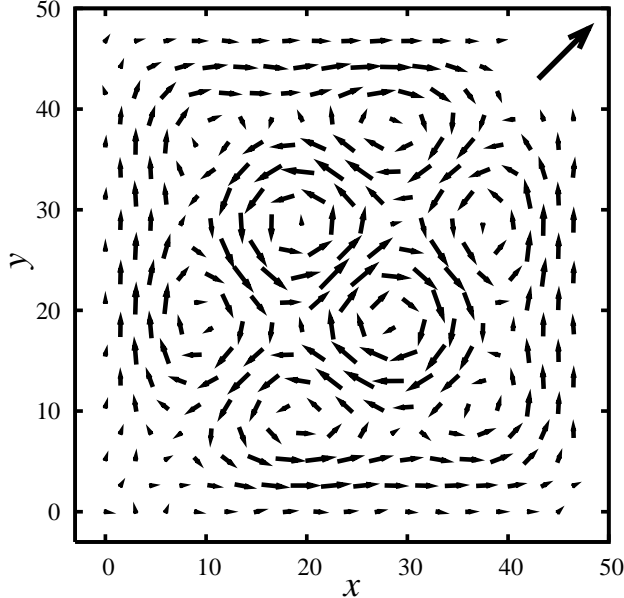


FIG. 4: Vortices in the distribution of the local field in a nearly square patch of a 2D triangular lattice of atoms at  $\delta = -1000$  and  $\delta_{LL} = -987.375$ . To avoid overcrowding of the plot, only one of each nine dipoles is shown. The incident light wave is polarized in the lattice plane along the diagonal of the lattice patch, its field is shown with a big arrow.

cases (c) and (d), for which  $\psi = 0$ :

$$q^2 = -\frac{8}{5} \frac{(\delta - \delta_{LL}) + i}{\delta_{LL}}. \quad (30)$$

By combining the cases (a) and (b) or the cases (c) and (d), we can achieve *simultaneous* size-related resonances, i. e., excitations of eigenmodes in both orthogonal directions in a patch of the 2D triangular lattice *at the same laser frequency*, if the patch is approximately square in shape. Resonances of the same order are hereby attained for locsitons with wave vectors pointing in the two orthogonal directions; a sufficient “squareness” of the lattice patch can be achieved by choosing its size (i. e., the numbers of atoms in the two directions). Locsitons with shorter wavelengths or with wave vectors pointing in different directions will be also present, but they will have no significant influence on the emerging dipole pattern due to their nonresonant nature.

Fig. 4 shows vector patterns that are formed by the atomic dipoles induced by the LF. The atoms are arranged in a  $48 \times 56$  patch of an equilateral triangular lattice, which results in approximately equal sides of the patch. The field of the incident electromagnetic wave is uniform and polarized along the diagonal of the patch and its frequency is close to the

electronic resonance of the two-level atom. The frequency of the incident wave is so chosen that the third size-related resonance (in the order of increasing wavenumbers, counting only those resonances allowed by the symmetry of the problem; for more detail see [2]) is excited in each dimension. Eight distinct vortices of the LF are visible in the plot. Fig. 4 only shows the imaginary parts of the complex field amplitudes, because they are dominant for each of the resonant locsitons. (We would like to note that a pair of vortices, apparently consistent with 2D-locsiton patterns originated by the 1-st locsiton resonance in our classification, was very recently observed in numerical simulations of plasmonic excitations in a 2D lattice of small metallic particles [17].)

### B. “Magic shapes”

As we noted in Sec. III A, the LF is “pushed out” of the lattice of strongly interacting dipoles at the exact atomic resonance [see Eq. (10)]. This effect, which we call the resonant LF suppression, represents a typical LF behavior at the atomic resonance; it is not limited to 2D lattices, but also occurs in 1D arrays of interacting atoms [1, 2] and in many finite 2D structures. We have shown earlier that in the 1D case, if a linear array of atoms is of a certain “magic size”, one encounters a *cancellation* of the resonant LF suppression, where one of the size-related locsitonic resonances partially restores the LF in the system [1, 2].

Finite 2D lattices and similar small systems of resonant atoms provide especially interesting examples of cancellation of the resonant LF suppression. Unlike in 1D arrays of atoms, the “restoration” of the LF in such systems at  $\delta = 0$ , compared to that in the uniform, Lorentz, case, can be more complete (up to 100%). Like in the 1D case [1, 2], the 2D “magic shapes” have a certain “cabbalistic” streak. For example, in the NNA the effect is most pronounced only in a system of  $N = 13$  atoms arranged as an equilateral six-point star with an atom at the center, for which the maximum restoration of the LF is reached,  $E_{\max}/E_{\text{in}} \approx 1.02$ . The directions and relative amplitudes of the LF at the atoms in this system are shown in Fig. 5(a) for  $\mathbf{E}_{\text{in}} \parallel \mathbf{u}_K$  and in Fig. 5(b)  $\mathbf{E}_{\text{in}} \perp \mathbf{u}_K$ . It is very notable that the system is “magic” for both orientations of the incident field. One can see from the picture that the LF is concentrated on the outermost atoms and the one at the center, while the LF at the inner hexagon of atoms is almost completely suppressed. This suppression is a manifestation of a special case of a locsiton standing eigenwave in a finite discrete atomic

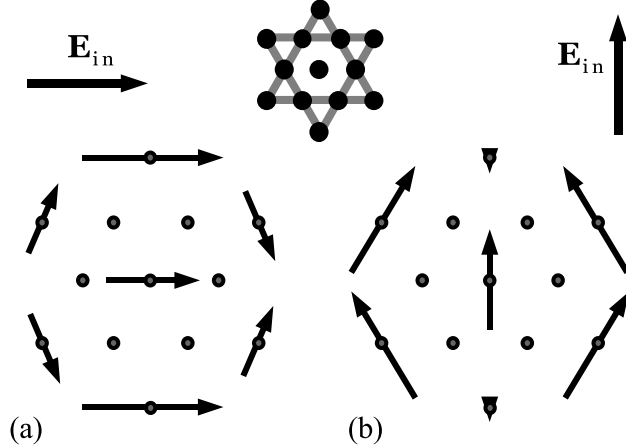


FIG. 5: “Magic” planar system of 13 resonant atoms for two different orientations of  $\mathbf{E}_{\text{in}}$  shown in plots (a) and (b). The inset illustrates the geometry of the system.

structure. (Within the NNA, the LF zeroes out at the “empty” atomic locations outside the outer hexagon, so locsitons make a 2D standing wave.) In general, the zeroes (nodes) of that wave are located somewhere in between atoms, so at each individual atom we have a nonzero LF amplitude. However, in the magic atomic configuration at the precise atomic resonance,  $\delta = 0$ , these nodes nearly coincide with the locations of the inner-hexagon atoms. Thus, we have a nearly ideal picture of a 2D standing wave, with large LF intensities at the antinodes (maxima), located at the central atom and the outer hexagon atoms, on one hand, and nodes (zeroes), located at the inner-hexagon atoms, on the other hand. To an extent, this situation is reminiscent of a 2D standing wave on a water surface in a round bucket with the first antinode at the center of the bucket, where some middle observation points are located at the nodes of the wave. Any symmetry distortion in this system (e. g., by attaching a foreign atom or molecule to it) would break the balance of the local fields in the system and bring back the resonant LF suppression, which is cancelled in the symmetric “magic system”. This effect could potentially lead to designing nanometer-scale sensors for detecting various biological molecules, etc. For example, such a nanodevice may include target-specific receptor molecules that form a locsiton-supporting “magic” system. A localized locsiton then would get suppressed whenever a target biomolecule attaches to a receptor, otherwise the locsiton suppression at the electronic resonance would be “magically” cancelled.

## V. LOCSITONS IN TRIANGULAR LATTICES: NORMAL POLARIZATION

The “ $\perp$ ” configuration, where the incident field is polarized at the normal to the lattice plane, may be realized, for example, by creating a standing wave by two counter-propagating laser beams with the beam axes lying in the lattice plane. For systems much smaller than the laser wavelength, the incident field may be then assumed nearly uniform. Locsitons emerging in the “ $\perp$ ” configuration are similar in many respects to 1D locsitons discussed in detail in [2], so here we only provide a brief overview of the “ $\perp$ ” case and outline the most distinctive features appearing in this geometry.

Let us start again with describing locsitons in unbounded lattices. The most general equation for the LF in the “ $\perp$ ” case is obtained from Eq. (4) by setting  $\mathbf{E}_{\text{in}}(\mathbf{r}) \parallel \mathbf{E}_{\text{L}}(\mathbf{r}) \perp \mathbf{u}$ :

$$\mathbf{E}_{\text{L}}(\mathbf{r}) = \mathbf{E}_{\text{in}}(\mathbf{r}) + \frac{Q}{4} \sum_{\text{lattice}}^{\mathbf{r}' \neq \mathbf{r}} \frac{l_a^3}{|\mathbf{r}' - \mathbf{r}|^3} \mathbf{E}_{\text{L}}(\mathbf{r}'). \quad (31)$$

As in the “ $\parallel$ ” case, we will assume here that the incident optical field is uniform,  $\mathbf{E}_{\text{in}}(\mathbf{r}) \equiv \mathbf{E}_{\text{in}}$ , which will help us to build a clearer understanding of the locsiton behavior in 2D lattices. For an equilateral triangular lattice, Eq. (31) can be simplified using the NNA as

$$\mathbf{E}_{\text{L}}(\mathbf{r}) = \mathbf{E}_{\text{in}} + \frac{Q}{4} \sum_{\mathbf{u}_{\text{K}}} \mathbf{E}_{\text{L}}(\mathbf{r} + l_a \mathbf{u}_{\text{K}}). \quad (32)$$

Equation (32) has a uniform, Lorentz, solution, which is given by Eq. (8) with  $\delta_{\text{LL}} = \delta_{\text{LL}}^{\perp}$  where

$$\delta_{\text{LL}}^{\perp} = \frac{3}{2} Q_a, \quad (33)$$

which is three times the NNA value for  $\delta_{\text{LL}}$  in a 1D array of atoms if  $\mathbf{E}_{\text{in}}$  is perpendicular to the array (and the dipoles are aligned “side-to-side”) [2]. This is a consequence of each atom having now 6 instead of 2 neighbors.

To obtain the corresponding dispersion relation  $\delta(\mathbf{q})$  for “ $\perp$ ” locsitons in the lattice, we substitute the LF  $\mathbf{E}_{\text{L}}(\mathbf{r})$  in Eq. (32) as a sum of the Lorentz solution given by Eqs. (8) and (33) and 2D plane-wave excitations (12). This dispersion relation can be written as

$$D_{2\perp}^{\text{NNA}}(\mathbf{q}) \equiv \frac{1}{3} \sum_{n=0}^2 \cos[q \cos(\theta_n - \psi)] = \frac{\delta + i}{\delta_{\text{LL}}^{\perp}}, \quad (34)$$

where, as in Sec. III B,  $\theta_n = \theta_0 + n\pi/3$ . In the long-wavelength limit,

$$D_{2\perp}^{\text{NNA}}(\mathbf{q}) \approx 1 - \frac{1}{4} q^2 + O(q^4), \quad (35)$$

so that the uniform, Lorentz, solution for the LF is reached at  $\delta = \delta_{\text{LL}}^{\perp}$ , where  $D_{2\perp}^{\text{NNA}}(\mathbf{q} = \mathbf{0}) = 1$ . The second term in the r.h.s. of Eq. (35) is independent of the orientation of  $\mathbf{q}$ , which means that no anisotropy caused by the lattice structure is present in the long-wavelength limit. We may thus conclude that, compared to the “||” case, the locsitons in the “ $\perp$ ” configuration are more reminiscent of the locsitons in 1D arrays of resonant atoms considered in [1, 2]. There is still no complete analogy here, as, e.g., the second term in the r.h.s. of Eq. (35) differs by a factor of 1/2 from the 1D result [2]. Moreover, dispersion relation (34) does become anisotropic for larger  $q$ , closer to the boundaries of the first Brillouin zone. This anisotropy, however, is by far less pronounced than that in the “||” case.

It is instructive to also obtain the dispersion relation in the NRA. By replacing the summation in Eq. (34) with an integration over the “near ring”, following the procedure outlined in Sec. III A, we get

$$1 - \frac{3Q}{2\pi} \int_0^\pi \cos[q \cos(\theta - \psi)] d\theta = 0. \quad (36)$$

The resulting dispersion relation turns out to be independent of the orientation of  $\mathbf{q}$ :

$$D_{2\perp}^{\text{NRA}}(\mathbf{q}) \equiv J_0(q) = \frac{\delta + i}{\delta_{\text{LL}}^{\perp}}, \quad (37)$$

which is not surprising given the NRA applicability in the long-wavelength limit.

While it might be somewhat harder to create a uniform incident field polarized normally to a 2D lattice, the resulting locsitons could be much easier to control because of the small anisotropy of the interatomic interactions in the “ $\perp$ ” geometry, compared to the “||” geometry. For example, defects in a 2D lattice can support *localized* locsitons, not unlike the *evanescent* 1D locsitons discussed in [2]. Compared to the complex locsiton patterns emerging in the “||” geometry [cf. Fig. 4] these localized locsitons are more likely to form well-organized strata-like patterns in the “ $\perp$ ” geometry.

Fig. 6 shows concentric dipole strata that are formed around a circular hole made by removing a few tens of atoms from a triangular lattice. The locsiton “attached” to the defect “decays” as the distance to the hole boundary increases, which is mostly a “diffraction” effect, although some contribution from the imaginary part of  $\mathbf{q}$  (like in evanescent 1D locsitons) is also present. In performing the numerical simulations for the plot, we made sure that the locsitons attached to the outside boundaries of the lattice patch (lying far outside the plotted region) do not interfere with the locsiton localized at the defect.

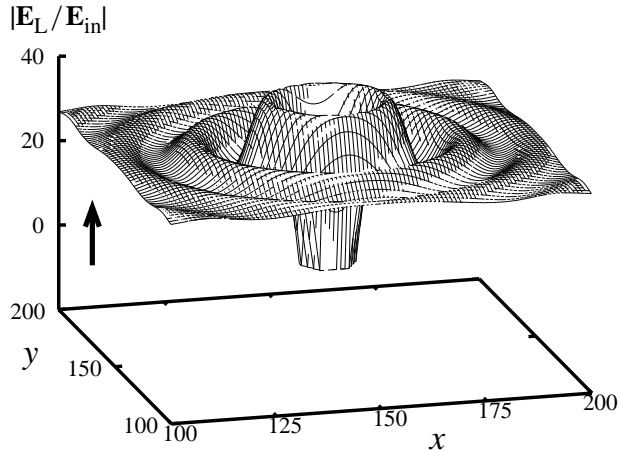


FIG. 6: Spatial strata of the normalized local field around a 15-point-wide hole in a 2D triangular lattice at  $\delta = 100$  and  $\delta_{LL} = 103.5$ . The direction of the incident field is shown with a big arrow.

## VI. CONCLUSIONS

In this paper we presented a detailed study of locsitons in nanoscale 2D lattices of resonant atoms with strong dipole interaction. These locsitons (i. e., excitations of the local field) and various associated effects were originally predicted in our recent publication [1]. Here, we have built analytic models for locsitons in infinite 2D triangular lattices of atoms, based either on the nearest-neighbor approximation or on the simpler near-ring approximation.

We have shown that the “in-plane” polarization geometry, where the incident laser field lies in the lattice plane, enables locsitons with the most unusual and diverse properties, as compared to the 1D case described in detail in [2]. In particular, the dispersion relations for the locsitons with an in-plane polarization are highly anisotropic with respect to the orientation of the locsiton polarization relative to its wave vector in the lattice plane, because of the highly anisotropic nature of the dipole-dipole interaction. We further demonstrated a method to design a finite 2D lattice, such that distinct vector locsiton patterns are formed at a certain laser frequency, the patterns containing multiple vortices in the local field distribution.

We have also considered a remarkable effect of a cancellation of the resonant local field suppression [1], which consists in the local field being able to penetrate certain “magic shapes” made of resonant atoms, despite the nearly-universal tendency of the local field to be “pushed out” of the lattice at the exact atomic resonance. In particular, we provided



more detail on the local field distribution in the simplest “magic shape” that can be cut out of a triangular lattice—a six-point star with an atom at the center.

In the case where the incident field is polarized normally to the lattice, we found that locsitons bear more analogy to locsitons in 1D arrays of atoms, compared to the case of an in-plane polarization. Finally, we illustrated the role of lattice defects in supporting localized locsitons.

While this paper does not elaborate on nonlinear effects involving 2D locsitons, to be addressed in our future publications, we note that, similarly to the 1D case [1, 2], our numerical simulations have shown optical bistability and hysteresis, which may be especially important for potential applications of 2D locsitons in designing all-dielectric nanoscale logic elements, devices for signal processing, etc.

### Acknowledgments

This work is supported by US AFOSR.

- 
- [1] A. E. Kaplan and S. N. Volkov, *Phys. Rev. Lett.* **101**, 133902 (2008).
  - [2] A. E. Kaplan and S. N. Volkov, *Phys. Rev. A* **79**, 053834 (2009).
  - [3] M. Born and E. Wolf, *Principles of Optics*, (Pergamon, Oxford, 1980), Ch. 2 and references therein.
  - [4] H. A. Lorentz, *Ann. Phys. Chem.* **9**, 641 (1880).
  - [5] L. Lorenz, *Ann. Phys. Chem.* **11**, 70 (1881).
  - [6] A. Aharoni, *Introduction to the Theory of Ferromagnetism* (Oxford Univ. Press, Oxford, 2001).
  - [7] C. Kittel, *Introduction to Solid State Physics* (Wiley, New York, 1996).
  - [8] V. M. Shalaev, W. Cai, U. K. Chettiar, H.-K. Yuan, A. K. Sarychev, V. P. Drachev, and A. V. Kildishev, *Opt. Lett.* **30**, 3356 (2005).
  - [9] V. A. Markel and A. K. Sarychev, *Phys. Rev. B* **75**, 085426 (2007).
  - [10] V. B. Sandomirskii, *Sov. Phys. JETP* **25**, 101 (1967).
  - [11] V. Chernyak, S. N. Volkov, and S. Mukamel, *Phys. Rev. Lett.* **86**, 995 (2001).

- [12] A. E. Kaplan, I. Marzoli, W. E. Lamb Jr., and W. P. Schleich, *Phys. Rev. A* **61**, 032101 (2000).
- [13] P. K. Ghosh, *Ion Traps* (Oxford Univ. Press, Oxford, 1996).
- [14] L. D. Landau and E. M. Lifshitz, *The Classical Theory of Fields* (Butterworth, New York, 1980).
- [15] J. J. Maki, M. S. Malcuit, J. E. Sipe, and R. W. Boyd, *Phys. Rev. Lett.* **67**, 972 (1991).
- [16] G. A. Korn and T. M. Korn, *Mathematical Handbook for Scientists and Engineers* (Dover, Mineola, New York, 2000).
- [17] S. V. Karpov and V. S. Gerasimov, private communication.